Polymer Journal (2010) 42, 735–744

www.nature.com/pj

ORIGINAL ARTICLE

A Monte Carlo study of the second virial coefficient of semiflexible ring polymers

Daichi Ida, Daisuke Nakatomi and Takenao Yoshizaki

A Monte Carlo (MC) study was made of the second virial coefficient A_2 of the ideal Kratky–Porod (KP) worm-like ring using a model composed of infinitely thin bonds with harmonic bending energy between successive bonds. Two kinds of statistical ensembles were generated: one composed of configurations of all kinds of knots with the Boltzmann weight, called the mixed ensemble, and the other composed of only those of the trivial knot, called the trivial-knot ensemble. The effective volume V_E excluded to one ring by the presence of another, resulting only from a topological interaction, and also the mean-square radius of gyration $\langle S^2 \rangle$ were evaluated for each ensemble. The dimensionless quantity $\lambda V_E/L^2$ proportional to A_2 was found to be a function only of the reduced total contour length λL, as in the case of $\lambda \langle S^2 \rangle /L$, where λ^{-1} is the stiffness parameter of the KP ring and L is its total contour length. The quantity $\lambda V_E/L^2$ first increased and then decreased after passing through a maximum at $\lambda L \simeq 5$, as λL was increased. A comparison with literature data for ring atactic polystyrene in cyclohexane at Θ shows that the present MC results may qualitatively explain the behavior of the data.
Polymer Journal (2010) **42,** 735–744; doi:10.1038/pj.2010.61; published online 21 July 2010

Keywords: MC simulation; second virial coefficient; semiflexible ring polymer; topological interaction

INTRODUCTION

Interaction between polymer chains, arising only from the chain connectivity (which inhibits chains from crossing each other), is important to understand not only the dynamical properties of concentrated solutions or melts but also static properties of solutions of ring polymers.[1,2] For ring polymers, this interaction is usually called a topological interaction (TI) because it works to conserve a given link type between a pair of ring polymers—it is a topological invariant. Consequently, a repulsive force, in the sense of the potential of mean force, results from the TI between unlinked ring polymers; therefore, the second virial coefficient A_2 remains positive even for the ideal rings without excluded volume, as explicitly shown in the Monte Carlo (MC) study made by Frank-Kamenetskii *et al.* using a lattice model.[3,4] Their pioneer work on A_2 of rings was followed by the theoretical studies of Iwata,[5,6] des Cloizeaux[7] and Tanaka,[8] and by the MC study of Deguchi and Tsurusaki[9] based on the Gaussian chain model, which is valid for very long, flexible ring polymers. We note that des Cloizeaux also calculated A_2 for the rigid ring.[7] Experimentally, positive values of A_2 were observed for ring atactic polystyrene (a-PS) in cyclohexane at the Θ temperature (34.5 or 35 °C) by Roovers and Toporowski,[10] by Huang *et al.*[11] and very recently by Takano *et al.*[12] in the range of weight-average molecular weight M_w from 1×10^4 to 6×10^5.

The effective volume V_E excluded to one ring by the presence of another is defined from A_2 by

$$A_2 = 4N_A V_E/M^2, \quad (1)$$

where N_A is the Avogadro constant and M is the molecular weight. The effective excluded volume may be considered proportional to the cube of the root-mean-square radius of gyration $\langle S^2 \rangle^{1/2}$ in both the rigid-ring and random-coil limits. Therefore, $V_E \propto L^3$ and $L^{3\nu}$ in the respective limits, where L is the total contour length of the ring and ν is the exponent in the asymptotic relation $\langle S^2 \rangle^{1/2} \propto L^\nu$ in the random-coil limit. The exponent ν is 1/2 for an ensemble constituted of rings of all kinds of knots with the Boltzmann weight and is considered $\sim$0.6 for one constituted of rings of the trivial knot (unknotted rings).[13,14] Thus, A_2 is proportional to M in the rigid-ring limit and to $M^{3\nu-2}$ ($M^{-1/2}$ or $M^{-0.2}$) in the random-coil limit, and must necessarily have a maximum in the range of the crossover from the rigid ring to the random coil. The purpose of this paper is to clarify such behavior of A_2 of the ideal ring in the crossover or, in other words, to examine the effect of chain stiffness on A_2 on the basis of the Kratky–Porod (KP) worm-like chain model.[15,16]

As analytical treatment of the TI is complicated even in the case of the Gaussian chain model,[5–8] we resorted to an MC approach using a model for semiflexible rings composed of infinitely thin bonds with a harmonic bending energy between successive bonds. We generated two kinds of statistical ensembles, that is, one composed of rings of all kinds of knots with the Boltzmann weight and the other composed of those only of the trivial knot, and compared the results for $\langle S^2 \rangle$ and A_2.

Department of Polymer Chemistry, Kyoto University, Kyoto, Japan
Correspondence: Dr T Yoshizaki, Department of Polymer Chemistry, Kyoto University, Katsura, Kyoto 615-8510, Japan.
E-mail: yoshizaki@molsci.polym.kyoto-u.ac.jp
Received 2 April 2010; revised 27 May 2010; accepted 28 May 2010; published online 21 July 2010

MATERIALS AND METHODS

Model

The MC model used in this study was essentially the same as that used by Frank-Kamenetskii *et al.*,[17] that is, a ring composed of infinitely thin n bonds of length l with a harmonic bending energy between successive bonds. The n joints in the ring were numbered 1, 2, $\cdots$, n from an arbitrary joint, and the ith bond vector from the ith joint to the $(i+1)$th was denoted by $\mathbf{l}_i$ ($i=1, 2, \cdots, n-1$); $\mathbf{l}_n$ was the nth bond vector from the nth joint to the first. The configuration of the ring could then be specified by the set $\{\mathbf{l}_n\}=[\mathbf{l}_1, \mathbf{l}_2, \cdots, \mathbf{l}_{n-1}, (\mathbf{l}_n)]$, apart from its position in an external Cartesian coordinate system. Note that $\mathbf{l}_n$ is a dependent variable for the ring. Let θ_i ($i=2, 3, \cdots, n$) be the angle between $\mathbf{l}_{i-1}$ and $\mathbf{l}_i$ and θ_1 be the angle between $\mathbf{l}_n$ and $\mathbf{l}_1$. The total potential energy U of the ring may be written in terms of θ_i as follows:

$$U(\{\mathbf{l}_n\}) = \frac{\alpha}{2}\sum_{i=1}^{n} \theta_i^2, \tag{2}$$

where α is the bending force constant. The MC model so defined becomes identical with the KP ring of total contour length L in the continuous limit $n\to\infty$, $l\to 0$, and $\langle \cos\theta_i\rangle \to 1$ under the conditions $nl=L$ and

$$l\frac{1+\langle\cos\theta\rangle}{1-\langle\cos\theta\rangle} = \lambda^{-1}, \tag{3}$$

where λ^{-1} is the stiffness parameter of the KP model and $\langle \cos\theta\rangle$ is defined as

$$\langle\cos\theta\rangle = \int_0^{\pi} \mathrm{e}^{-\alpha\theta^2/2k_\mathrm{B}T}\cos\theta\,\sin\theta\,\mathrm{d}\theta \Big/ \int_0^{\pi} \mathrm{e}^{-\alpha\theta^2/2k_\mathrm{B}T}\sin\theta\,\mathrm{d}\theta \tag{4}$$

with k_B the Boltzmann constant and T the absolute temperature.[17,18] Note that the MC model reduces to the freely jointed chain in the limit of $\alpha\to 0$.

In what follows, we set $l=1$ for simplicity and carried out MC simulations for the rings with values of $\alpha/k_\mathrm{B}T$ given in the first column of Table 1. The values of $\langle\cos\theta\rangle$ calculated from Equation (4) and those of λ^{-1} of the corresponding KP model calculated from Equation (3) with $l=1$ are given in the second and third columns, respectively.

MC sampling

For the initial configuration $\{\mathbf{l}_n\}$, we adopted an n-sided regular polygon of unit side length, which is the most stable configuration, and sequentially deformed it by the virtual motion introduced by Deutsch.[19] We let $\mathbf{v}$ be the unit vector along the vector distance between a pair of joints randomly chosen under the condition that they not be next to each other. If the ith and jth joints ($i<j$) were chosen, $\mathbf{v}$ was along the vector sum $\sum_{k=i}^{j-1}\mathbf{l}_k$. As illustrated in Figure 1, a trial configuration $\{\mathbf{l}'_n\}$ was generated by rotating the shorter part of the ring around $\mathbf{v}$ by an angle ϕ randomly chosen in the range of $[-\pi, \pi)$. The bond vectors $\mathbf{l}_i, \mathbf{l}_{i+1}, \cdots, \mathbf{l}_{j-1}$ were rotated if $j-i\leqslant n/2$ and the rest otherwise. If the bond vector $\mathbf{l}_k$ underwent the rotation, $\mathbf{l}'_k$ could be given by[20]

$$\begin{aligned}\mathbf{l}'_k &= \mathbf{v}\mathbf{v}\cdot\mathbf{l}_k + (\cos\phi)(\mathbf{I}-\mathbf{v}\mathbf{v})\cdot\mathbf{l}_k + (\sin\phi)\mathbf{v}\times\mathbf{l}_k \\ &\equiv \mathbf{R}(\mathbf{v};\,\phi)\cdot\mathbf{l}_k,\end{aligned} \tag{5}$$

where $\mathbf{I}$ is the unit matrix and the rotation matrix $\mathbf{R}(\mathbf{v};\,\phi)$ is given by

$$\begin{aligned}\mathbf{R}(\mathbf{v};\,\phi) =& (\cos\phi)\mathbf{I} + (1-\cos\phi)\begin{pmatrix} v_x^2 & v_xv_y & v_xv_z \\ v_yv_x & v_y^2 & v_yv_z \\ v_zv_x & v_zv_y & v_z^2 \end{pmatrix} \\ &+ \sin\phi\begin{pmatrix} 0 & -v_z & v_y \\ v_z & 0 & -v_x \\ -v_y & v_x & 0 \end{pmatrix}\end{aligned} \tag{6}$$

with v_x, v_y, v_z the Cartesian components of $\mathbf{v}$ in an external system. With this rotation, $\mathbf{l}'_k$ was renormalized to $\mathbf{l}'_{k\,(\mathrm{corr})}$ so that $|\mathbf{l}'_{k\,(\mathrm{corr})}|=1$, that is,

$$\mathbf{l}'_{k(\mathrm{corr})} = \mathbf{l}'_k/|\mathbf{l}'_k| \simeq [1-\tfrac{1}{2}(|\mathbf{l}'_k|^2-1)]\mathbf{l}'_k. \tag{7}$$

This was carried out to suppress roundoff errors characteristic of computer work. (Note that $|\mathbf{l}'_k-\mathbf{l}'_{k\,(\mathrm{corr})}|\ll 1$.) If the bond vector $\mathbf{l}_k$ did not undergo the rotation, on the other hand, we had $\mathbf{l}'_k=\mathbf{l}_k$.

Then, the adoption of the next trial configuration $\{\mathbf{l}'_n\}$ was determined by the Metropolis method of importance sampling[21] on the basis of the total potential energies given by Equation (2) for $\{\mathbf{l}'_n\}$ and $\{\mathbf{l}_n\}$. That is, $\{\mathbf{l}'_n\}$ was adopted as the next configuration with the (transition) probability $\tau(\{\mathbf{l}'_n\}|\{\mathbf{l}_n\})$ defined as

$$\tau(\{\mathbf{l}'_n\}|\{\mathbf{l}_n\}) = \min(1,\, \mathrm{e}^{-\Delta U/k_\mathrm{B}T}) \tag{8}$$

with ΔU given by

$$\Delta U = U(\{\mathbf{l}'_n\}) - U(\{\mathbf{l}_n\}) = \frac{\alpha}{2}(\theta_i'^2+\theta_j'^2-\theta_i^2-\theta_j^2), \tag{9}$$

where θ'_i ($i=2, 3, \cdots, n$) is the angle between $\mathbf{l}'_{i-1}$ and $\mathbf{l}'_i$ and θ'_1 the angle between $\mathbf{l}'_n$ and $\mathbf{l}'_1$. If $\{\mathbf{l}'_n\}$ was discarded, $\{\mathbf{l}_n\}$ was again adopted as the next configuration.

Through this MC algorithm, we sampled one configuration at every M_nom (nominal) steps and N_s configurations in total after an equilibration of $10^4\times M_\mathrm{nom}$ steps. As each MC step did not conserve a knot type, the ensemble so obtained was composed of N_s configurations of all kinds of knots with the Boltzmann weight. We call this ensemble the *mixed ensemble*. Following the procedure of Vologodskii *et al.*[22] to distinguish the trivial knot from the others using the Alexander polynomial,[23] we extracted configurations of the trivial knot from the mixed ensemble and evaluated the ratio $f_\mathrm{t.k.}$ of the number of the configurations to N_s. Unfortunately, however, this procedure could not exclude all the nontrivial knots, for example, the Kinoshita–Terasaka knot having 11 crossings.[24] Nevertheless, we accepted the values of $f_\mathrm{t.k.}$ so evaluated, considering that the number of residual nontrivial knots could be very small, if any existed.

Table 1 Values of $\langle\cos\theta\rangle$ and λ^{-1}

$\alpha/k_B\mathrm{T}$	$\langle\cos\theta\rangle$	λ^{-1}
0	0	1
0.3	0.1695	1.408
1	0.4406	2.575
3	0.7305	6.421
10	0.9064	20.36
30	0.9674	60.34
100	0.9901	200.3

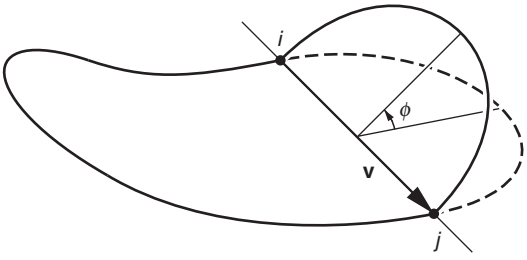

Figure 1 Illustration of an elementary step in MC simulations.

To make a *trivial-knot ensemble*, in addition to the mixed ensemble, N_s configurations of the trivial knot were extracted from many mixed ensembles by the above procedure. Although this trivial-knot ensemble inevitably included residual nontrivial knots, we ignored their contribution as in the case of the evaluation of $f_{t.k.}$.

It should be noted here that a possible roundoff error in numerical processes might violate the ring-closure condition,

$$\sum_{i=1}^{n} \mathbf{l}_i = \mathbf{0}. \tag{10}$$

Therefore, we confirmed that the absolute value of the vector sum on the left-hand side of Equation (10) did not exceed 10^{-9} for every configuration.

All numerical work was carried out using a personal computer with an Intel Core i7-860 CPU (Intel, Santa Clara, CA, USA). A source program coded in C was compiled by the GNU C compiler version 4.5.0 (Free Software Foundation, Inc., Boston, MA, USA) with real variables of double precision. For the generation of pseudorandom numbers, the subroutine package MT19937 supplied by Matsumoto and Nishimura[25] was used instead of the subroutine RAND included in the standard C library.

Mean-square radius of gyration

The mean-square radius of gyration $\langle S^2 \rangle$, that is, the ensemble average of the square radius of gyration S^2 as a function of $\{\mathbf{l}_n\}$, could be evaluated from

$$\langle S^2 \rangle = N_s^{-1} \sum_{\{\mathbf{l}_n\}} \left[\frac{1}{n} \sum_{i=1}^{n} |\mathbf{S}_i(\{\mathbf{l}_n\})|^2 \right], \tag{11}$$

where the sum is taken over N_s configurations in a given ensemble and $\mathbf{S}_i$ is the vector distance from the center of mass of the ring to the ith joint given by

$$\mathbf{S}_i = (1 - \delta_{i1}) \sum_{j=1}^{i-1} \mathbf{l}_j - \frac{1}{n} \sum_{j=1}^{n-1} \sum_{k=1}^{j} \mathbf{l}_k \tag{12}$$

with δ_{ij} the Kronecker delta. In what follows, $\langle S^2 \rangle_{mix}$ and $\langle S^2 \rangle_{t.k.}$ denote $\langle S^2 \rangle$'s calculated from Equations (11) and (12) using the mixed and trivial-knot ensembles, respectively.

Second virial coefficient

To evaluate the intermolecular potential energy resulting from the TI between two unlinked rings, a proper method was needed to determine whether the two rings were linked (nontrivial link) or not (trivial link). Two methods are available. One is based on the Alexander polynomial for links of two components,[26] which is more reliable but less feasible and was adopted by Frank-Kamenetskii *et al.*[3,4] and Deguchi and Tsurusaki.[9] The other is based on the Gauss linking number Lk,[26] which is more feasible but less reliable and was adopted by Iwata,[5,6] des Cloizeaux[7] and Tanaka.[8] We note that Lk of some kinds of nontrivial links, including the so-called Whitehead link,[26] vanishes as in the case of the trivial link.[26] In this study, we adopted the latter method to save computation time.

We considered a pair of rings 1 and 2 and let $\mathbf{r}_{i_p}(x_p)$ be the vector position of the contour point on the i_pth bond vector $\mathbf{l}_{i_p}$ (i_p=1, 2, ⋯, n) of ring p (p=1, 2), with the contour distance from the i_pth joint being x_p ($0 \leqslant x_p < 1$). The vector $\mathbf{r}_{i_p}(x_p)$ is given by

$$\mathbf{r}_{i_p}(x_p) = x_p \mathbf{l}_{i_p} + \mathbf{S}_{i_p} + \mathbf{r}_{c.m.,p}, \tag{13}$$

where $\mathbf{S}_{i_p}$, in turn, is given by Equation (12) and $\mathbf{r}_{c.m.,p}$ is the vector position of the center of mass of ring p. The Gauss linking number Lk for the pair of rings 1 and 2 could then be written in the form,

$$Lk = \frac{1}{4\pi} \sum_{i_1=1}^{n} \sum_{i_2=1}^{n} C_{i_1 i_2}, \tag{14}$$

where $C_{i_1 i_2}$ is defined by

$$C_{i_1 i_2} = \int_0^1 \int_0^1 \frac{(\mathbf{l}_{i_1} \times \mathbf{l}_{i_2}) \cdot [\mathbf{r}_{i_2}(x_2) - \mathbf{r}_{i_1}(x_1)]}{|\mathbf{r}_{i_2}(x_2) - \mathbf{r}_{i_1}(x_1)|^3} \mathrm{d}x_1 \mathrm{d}x_2. \tag{15}$$

Integration over x_1 and x_2 led to[27]

$$C_{i_1 i_2} = F(a_1, a_2) + F(a_1+1, a_2+1) - F(a_1+1, a_2) - F(a_1, a_2+1) \tag{16}$$

with $F(x, y)$ given by

$$F(x, y) = \arctan \left[\frac{xy + a_3^2 \cos \theta_{i_1 i_2}}{a_3 (x^2 + y^2 - 2xy \cos \theta_{i_1 i_2} + a_3^2 \sin^2 \theta_{i_1 i_2})^{1/2}} \right], \tag{17}$$

where $\theta_{i_1 i_2}$ is the angle between $\mathbf{l}_{i_1}$ and $\mathbf{l}_{i_2}$ and a_1, a_2 and a_3 in Equations (16) and (17) are given by

$$\begin{aligned} a_1 &= -(\sin \theta_{i_1 i_2})^{-2} (\mathbf{S}_{i_2} - \mathbf{S}_{i_1} + \mathbf{r}) \cdot (\mathbf{l}_{i_1} - \mathbf{l}_{i_2} \cos \theta_{i_1 i_2}), \\ a_2 &= (\sin \theta_{i_1 i_2})^{-2} (\mathbf{S}_{i_2} - \mathbf{S}_{i_1} + \mathbf{r}) \cdot (\mathbf{l}_{i_2} - \mathbf{l}_{i_1} \cos \theta_{i_1 i_2}), \\ a_3 &= (\sin \theta_{i_1 i_2})^{-2} (\mathbf{S}_{i_2} - \mathbf{S}_{i_1} + \mathbf{r}) \cdot (\mathbf{l}_{i_1} \times \mathbf{l}_{i_2}) \end{aligned} \tag{18}$$

with $\mathbf{r} = \mathbf{r}_{c.m.,2} - \mathbf{r}_{c.m.,1}$ the vector distance between the two centers of mass.

The potential energy U_{12} between rings 1 and 2 is explicitly defined, using the McMillan–Mayer symbolism,[28,29] as

$$\begin{aligned} U_{12}(1, 2) &= 0 \quad \text{if } Lk = 0 \\ &= \infty \quad \text{otherwise,} \end{aligned} \tag{19}$$

and the averaged intermolecular potential (potential of mean force) $\overline{U}_{12}(r)$ as a function of the distance $r = |\mathbf{r}|$ between the centers of mass of rings 1 and 2 is defined by

$$\overline{U}_{12}(r) = -k_B T \ln \left\langle \exp \left[-\frac{U_{12}(1, 2)}{k_B T} \right] \right\rangle_r. \tag{20}$$

In Equation (20), $\langle \cdots \rangle_r$ indicates the conditional equilibrium average over the configurations of the two rings with $\mathbf{r}$ fixed using the single-ring distribution function for each and the bending potential energy given by Equation (2). The second virial coefficient A_2 may be written in terms of $\overline{U}_{12}(r)$ as follows,

$$A_2 = \frac{2\pi N_A}{M^2} \int_0^\infty \left\{ 1 - \exp \left[-\frac{\overline{U}_{12}(r)}{k_B T} \right] \right\} r^2 \mathrm{d}r. \tag{21}$$

In practice, $\exp[-\overline{U}_{12}(r)/k_B T]$, that is, the conditional average on the right-hand side of Equation (20), was evaluated as a function of r for each ensemble constituted of N_s configurations. First, we randomly chose a pair of configurations (rings 1 and 2) from the N_s configurations and randomized their orientations in the external coordinate system. To obtain $\exp[-\overline{U}_{12}(1, 2)/k_B T] = \delta_{0,Lk}$, we then calculated Lk for the pair at given r from Equation (14) with Equations (16)–(18). Finally, we determined the value of $\exp[-\overline{U}_{12}(r)/k_B T]$ to be $N_{t.l.}/N_p$, where N_p is the total number of sample pairs and $N_{t.l.}$ is the number of the trivial links (Lk=0) included in the N_p pairs.

With the values of $\exp[-\overline{U}_{12}(r)/k_B T]$ so obtained for various values of r, the effective volume V_E could then be calculated from Equation (1) with Equation (21) by numerical integration applying

the trapezoidal rule formula. As in the case of $\langle S^2 \rangle$, V_E's obtained for the mixed and trivial-knot ensembles are denoted by $V_{E,mix}$ and $V_{E,t.k.}$, respectively.

RESULTS AND DISCUSSION

We carried out MC simulations for polymer rings with the values α/k_BT given in the first column of Table 1 and with n=10, 20, 50, 100 and 200. Extra MC simulations were carried out for the rings with α/k_BT=0 (freely jointed chain) and for n=500 and 1000. To keep the mean number of (real) configurational changes at every M_{nom} (nominal) steps nearly equal to n, we set $M_{nom}=n$ for α/k_BT=0, $M_{nom} \simeq 2n$ for α/k_BT=0.3 and 1, $M_{nom} \simeq 5n$ for α/k_BT=3 and 10, and $M_{nom} \simeq 10n$ for α/k_BT=30 and 100. Five mixed and five trivial-knot ensembles were then constructed for each case of α/k_BT and n, each constituted of 10^5 ($=N_s$) configurations except for α/k_BT=0 and n=1000. For that case, each ensemble was constituted of 10^4 configurations. We note that many mixed ensembles were constructed to extract 10^5 (or 10^4) configurations of the trivial knot from them. To determine A_2 [or $\exp(-\overline{U}_{12}/k_BT)$], 10^6 ($=N_p$) pairs of configurations were chosen from each ensemble.

Fraction of the trivial knots

The ratio $f_{t.k.}$ of the number of configurations of the trivial knot included in a given mixed ensemble to the total number N_s of configurations in the ensemble was evaluated. The values of $f_{t.k.}$ and its statistical error are given in the second column of Table 2 as the mean and s.d., respectively, of five independent MC results for given values of α/k_BT and n.

Figure 2 shows plots of $f_{t.k.}$ against the logarithm of the *reduced* total contour length λL, that is, the total contour length $L=n$ divided by the stiffness parameter λ^{-1}. The open circles represent the MC values for α/k_BT=0 (pip up), 0.3 (pip right-up), 1 (pip right), 3 (pip right-down), 10 (pip down), 30 (pip left-down) and 100 (pip left). For comparison, the MC values (dot) obtained by Moore *et al.*[14] are shown for rings with α/k_BT=0 in the range of $n(=\lambda L)$ from 15 to 3000. We note that Moore *et al.*[14] adopted the procedure for extracting configurations of the trivial knot proposed by Deguchi and Tsurusaki[9] using not only the Alexander polynomial but also the Vassiliev invariants[30] of degree 2 and 3. The data points for various values of α/k_BT along with those of Moore *et al.* seem to form a single-composite curve, indicating that $f_{t.k.}$ is a function only of λL. It is interesting to note that $f_{t.k.}$ is almost equal to unity up to $\lambda L \simeq 10$ and then monotonically decreases to zero with increasing λL, and finally seems to vanish as predicted by Diao *et al.*[31,32]

The agreement of $f_{t.k.}$ as a function of λL between the present MC results and those of Moore *et al.* indicates that the present MC method for constructing mixed ensembles and the procedure for extracting configurations of the trivial knot from the ensembles works satisfactorily.

Mean-square radius of gyration

The mean-square radii of gyration $\langle S^2 \rangle_{mix}$ and $\langle S^2 \rangle_{t.k}$ were calculated from Equation (11) with Equation (12) for all mixed and trivial-knot ensembles, respectively. The values of $\langle S^2 \rangle_{mix}/n$ and its statistical error are given in the third column of Table 2 as the mean and s.d., respectively, of five independent MC results for given values of α/k_BT and n. The fifth column gives values of $\langle S^2 \rangle_{t.k}/n$ and its statistical error evaluated in the same manner.

Figure 3 shows double-logarithmic plots of $\lambda\langle S^2 \rangle/L$ ($=\lambda\langle S^2 \rangle/n$) against λL. The open and closed circles represent $\lambda\langle S^2 \rangle_{mix}/L$ and $\lambda\langle S^2 \rangle_{t.k}/L$, respectively; the various directions of pips carry the same meaning as those in Figure 2. The solid curve represents the theoretical values of $\lambda\langle S^2 \rangle_{mix}/L$ for the KP ring calculated from the following:[16,18,33]

$$\frac{\lambda\langle S^2\rangle_{mix}}{L} = \frac{\lambda L}{4\pi^2}[1 - 0.1140\lambda L - 0.0055258(\lambda L)^2 + 0.0022471(\lambda L)^3 - 0.00013155(\lambda L)^4 \quad \text{for } \lambda L \leqslant 6$$
$$= \frac{1}{12}\left\{1 - \frac{7}{6\lambda L} - 0.025\exp[-0.01(\lambda L)^2]\right\} \quad \text{for } \lambda L > 6. \tag{22}$$

The KP theory of $\langle S^2 \rangle_{mix}$ is for the so-called phantom chain, and its value becomes $L^2/4\pi^2$ in the rigid-ring limit and $\lambda^{-1}L/12$ in the random-coil limit.[29,34,35] All MC values of $\lambda\langle S^2 \rangle_{mix}/L$, except those for $\alpha/k_BT \leqslant 1$ and $n \leqslant 20$, seem to form a single-composite curve and to agree almost completely with the KP theory values. This is an

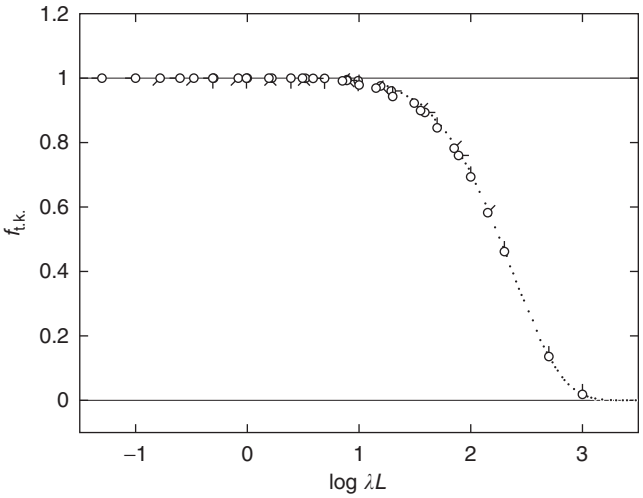

Figure 2 Plots of $f_{t.k.}$ against log λL. The open circles represent the present MC values, with various directions of pips indicating different values of α/k_BT: pip up, 0; successive 45° rotations clockwise correspond to 0.3, 1, 3, 10, 30 and 100, respectively. The dots represent the values obtained by Moore *et al.*[14]

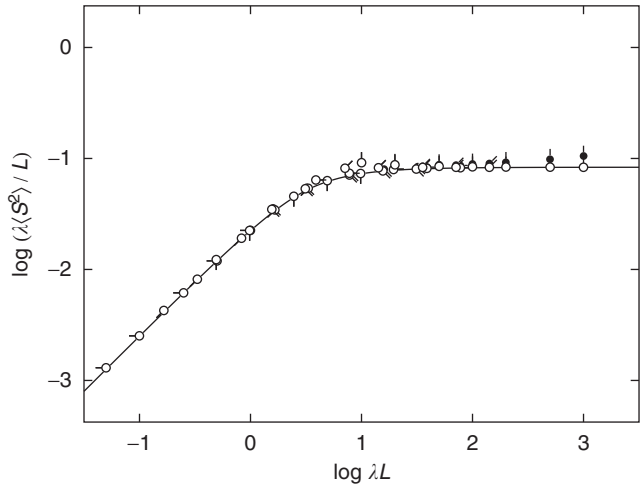

Figure 3 Double-logarithmic plots of $\lambda\langle S^2 \rangle/L$ against λL. The open and closed circles represent the values of $\lambda\langle S^2 \rangle_{mix}/L$ and $\lambda\langle S^2 \rangle_{t.k.}/L$, respectively, and the solid curve represents the KP theory values.[16,18,33] Various directions of pips attached to the circles carry the same meaning as those in Figure 2.

Table 2 Values of $f_{t.k.}$, $\langle S^2\rangle/n$, and V_E/n^2

n	$10^2 f_{t.k.}$ (error %)	$\langle S^2\rangle_{mix}/n$ (error %)	$10^2 V_{E,mix}/n^2$ (error %)	$\langle S^2\rangle_{t.k.}/n$ (error %)	$10^2 V_{E,t.k.}/n^2$ (error %)
$\alpha/k_BT=0$					
10	97.8_5 (0.1)	0.0916_5 (0.1)	0.578_9 (0.2)	0.0921_1 (0.1)	0.583_3 (0.4)
20	94.2_1 (0.1)	0.0875_6 (0.2)	0.568_8 (0.5)	0.0886_5 (0.2)	0.577_1 (0.3)
50	84.5_9 (0.1)	0.0849_9 (0.2)	0.498_1 (0.4)	0.0878_6 (0.2)	0.513_4 (0.4)
100	69.3_6 (0.1)	0.0841_1 (0.2)	0.424_7 (0.4)	0.0891_5 (0.1)	0.448_3 (0.4)
200	41.1_9 (0.3)	0.0838_0 (0.1)	0.349_6 (0.2)	0.0921_9 (0.2)	0.383_8 (0.2)
500	13.5_9 (0.0)	0.0834_9 (0.2)	0.258_9 (0.0)	0.0982_6 (0.0)	0.304_0 (0.0)
1000	1.8_4 (0.0)	0.0833_6 (0.2)	0.201_5 (0.3)	0.105_0 (0.2)	0.253_4 (0.2)
$\alpha/k_BT=0.3$					
10	99.1_6 (0.0)	0.115_0 (0.2)	0.829_5 (0.5)	0.115_2 (0.2)	0.831_6 (0.5)
20	96.9_2 (0.1)	0.116_2 (0.2)	0.835_3 (0.4)	0.117_1 (0.2)	0.840_8 (0.4)
50	89.9_5 (0.1)	0.116_9 (0.2)	0.750_0 (0.4)	0.119_7 (0.2)	0.768_9 (0.4)
100	78.2_4 (0.2)	0.117_3 (0.2)	0.654_4 (0.3)	0.122_7 (0.1)	0.681_2 (0.3)
200	58.2_5 (0.2)	0.117_3 (0.1)	0.546_0 (0.3)	0.126_6 (0.1)	0.586_4 (0.3)
$\alpha/k_BT=1$					
10	99.9_3 (0.0)	0.164_8 (0.1)	1.53_2 (0.4)	0.164_8 (0.1)	1.53_6 (0.4)
20	99.2_9 (0.0)	0.189_4 (0.1)	1.62_1 (0.3)	0.189_8 (0.1)	1.62_3 (0.4)
50	96.0_2 (0.0)	0.205_0 (0.2)	1.53_8 (0.2)	0.207_1 (0.2)	1.55_3 (0.3)
100	89.3_5 (0.1)	0.209_8 (0.1)	1.37_8 (0.4)	0.215_2 (0.2)	1.41_1 (0.3)
200	76.0_1 (0.1)	0.212_1 (0.1)	1.18_4 (0.2)	0.222_8 (0.1)	1.24_0 (0.2)
$\alpha/k_BT=3$					
10	100	0.223_4 (0.0)	2.86_6 (0.6)	0.223_4 (0.0)	2.86_1 (0.3)
20	99.9_8 (0.0)	0.342_5 (0.1)	3.97_4 (0.4)	0.342_6 (0.2)	3.98_1 (0.6)
50	99.5_1 (0.0)	0.455_0 (0.4)	4.19_4 (0.6)	0.456_1 (0.3)	4.20_3 (0.5)
100	97.5_6 (0.1)	0.495_5 (0.2)	4.00_6 (0.5)	0.499_4 (0.2)	4.02_5 (0.4)
200	92.2_7 (0.1)	0.515_4 (0.1)	3.62_8 (0.3)	0.526_1 (0.1)	3.70_0 (0.3)
$\alpha/k_BT=10$					
10	100	0.249_7 (0.0)	3.62_3 (0.4)	0.249_7 (0.0)	3.62_9 (0.3)
20	100	0.457_3 (0.0)	6.77_5 (0.3)	0.457_4 (0.0)	6.75_4 (0.4)
50	99.9_8 (0.0)	0.929_5 (0.1)	11.9_9 (0.6)	0.929_4 (0.1)	12.0_1 (0.5)
100	99.9_1 (0.0)	1.28_3 (0.2)	13.4_2 (0.5)	1.28_5 (0.2)	13.4_3 (0.3)
200	99.1_9 (0.0)	1.49_0 (0.2)	13.2_5 (0.4)	1.49_3 (0.1)	13.3_0 (0.5)
$\alpha/k_BT=30$					
10	100	0.257_7 (0.0)	3.88_0 (0.2)	0.257_7 (0.0)	3.87_7 (0.5)
20	100	0.492_4 (0.0)	7.75_3 (0.4)	0.492_4 (0.0)	7.76_6 (0.4)
50	99.9_9 (0.0)	1.15_2 (0.1)	17.6_4 (0.4)	1.15_2 (0.1)	17.6_7 (0.6)
100	99.9_8 (0.0)	2.07_3 (0.0)	29.2_8 (0.3)	2.07_3 (0.1)	29.3_1 (0.4)
200	99.9_7 (0.0)	3.25_2 (0.2)	38.6_1 (0.4)	3.25_3 (0.2)	38.7_2 (0.6)
$\alpha/k_BT=100$					
10	100	0.260_6 (0.0)	3.96_6 (0.3)	0.260_6 (0.0)	3.97_6 (0.2)
20	100	0.505_2 (0.0)	8.15_8 (0.3)	0.505_2 (0.0)	8.16_4 (0.2)
50	100	1.23_3 (0.1)	19.9_8 (0.3)	1.23_3 (0.1)	19.9_8 (0.3)
100	99.9_9 (0.0)	2.39_2 (0.0)	37.9_5 (0.3)	2.39_2 (0.0)	37.9_3 (0.2)
200	99.9_8 (0.0)	4.50_3 (0.1)	67.8_7 (0.5)	4.50_3 (0.1)	68.0_0 (0.4)

indication that the present MC method for constructing mixed ensembles works satisfactorily. The values for $\alpha/k_BT \leqslant 1$ and $n \leqslant 20$ are somewhat dispersed because of chain discreteness. It is interesting to see that $\lambda\langle S^2\rangle_{t.k.}/L$ deviates upward gradually from $\lambda\langle S^2\rangle_{mix}/L$ as λL is increased from ~ 10, where $f_{t.k.}$ begins to decrease from unity. Note that the dimensions of the ring of the trivial knot ought to be larger than those of nontrivial knots.

It is seen from Figure 3 that the intramolecular topological constraint, which makes the ring preserve the trivial knot, works in the same manner as the intramolecular excluded-volume effect.[7,13] In light of this observation, we examined the behavior of a kind of expansion factor defined by $\langle S^2\rangle_{t.k}/\langle S^2\rangle_{mix}$ as a function of λL. Figure 4 shows double-logarithmic plots of $\langle S^2\rangle_{t.k}/\langle S^2\rangle_{mix}$ against λL. The closed circles represent the values $\langle S^2\rangle_{t.k}/\langle S^2\rangle_{mix}$

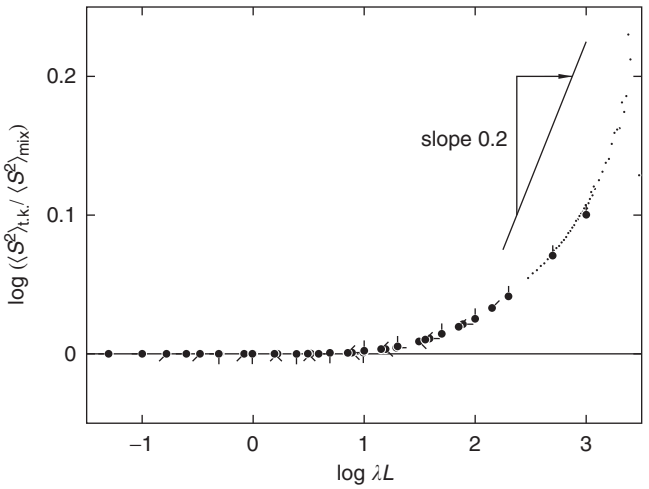

Figure 4 Double-logarithmic plots of $\langle S^2\rangle_{t.k.}/\langle S^2\rangle_{mix}$ against λL. The closed circles represent the MC values, with various directions of pips carrying the same meaning as those in Figure 2. The dots represent the values obtained by Moore *et al.*[14]

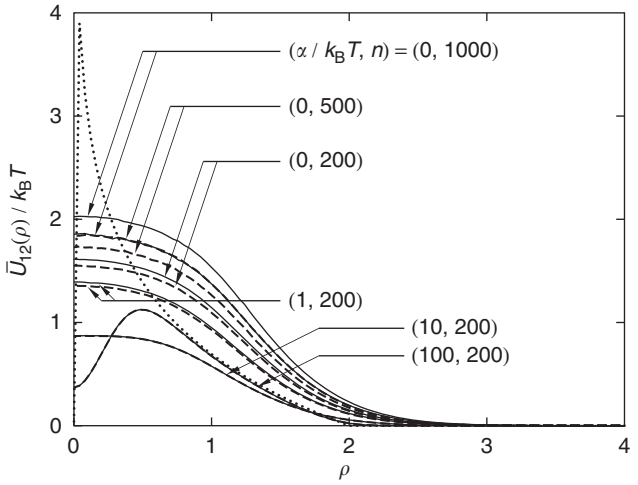

Figure 5 Plots of $\overline{U}_{12}(\rho)/k_BT$ against ρ for a pair of rings with the indicated values of α/k_BT and n. The solid and dashed line segments connect the values for the mixed and trivial-knot ensembles, respectively, and the dotted line segments connect those for a pair of 200-sided regular polygons.

calculated from the MC values $\langle S^2\rangle_{mix}/n$ and $\langle S^2\rangle_{t.k.}/n$ given in the third and fifth columns of Table 2; the various directions of pips carry the same meaning as those in Figure 2. For comparison, the MC values (dot) obtained by Moore *et al.*[14] for rings with $\alpha/k_BT=0$ in the range of $n(=\lambda L)$ from 300 to 3000 are also shown. The data points for various values of α/k_BT along with those of Moore *et al.* seem to form a single-composite curve, indicating that $\langle S^2\rangle_{t.k.}/\langle S^2\rangle_{mix}$ is also a function only of λL. As a natural consequence of the behavior of $f_{t.k.}$ shown in Figure 2, $\langle S^2\rangle_{t.k.}/\langle S^2\rangle_{mix}$ is almost equal to unity up to $\lambda L\simeq 10$, then monotonically increases with increasing λL. Although $\langle S^2\rangle_{t.k.}/\langle S^2\rangle_{mix}$ is considered to become proportional to L^{ν} ($\nu\simeq 0.2$) in the random-coil limit,[13,14] it is difficult to derive a definite conclusion from only the present data for $\lambda L\leqslant 10^3$.

The agreement of $\langle S^2\rangle_{t.k.}/\langle S^2\rangle_{mix}$ as a function of λL between the present MC results and those of Moore *et al.* reconfirms the validity of the present MC method for constructing mixed ensembles and the procedure for extracting configurations of the trivial knot from the ensembles.

Second virial coefficient

We first examined the behavior of the average intermolecular potential $\overline{U}_{12}$ as a function of the reduced distance $\rho=r\langle S^2\rangle^{-1/2}$ between the centers of mass of rings 1 and 2; r is the distance between the centers of mass of the two rings. For both the mixed and the trivial-knot ensembles with given values of α/k_BT and n, $\overline{U}_{12}/k_BT$ was evaluated for various values of ρ. We note that the values of $\langle S^2\rangle_{mix}$ and $\langle S^2\rangle_{t.k.}$ given in Table 2 were used in the determination of ρ for the mixed and trivial-knot ensembles, respectively.

Figure 5 shows plots of $\overline{U}_{12}(\rho)/k_BT$ against ρ for pairs of rings with the indicated values of α/k_BT and n. The solid and dashed line segments connect the values for the mixed and trivial-knot ensembles, respectively. For comparison, we also show the values for a pair of 200-sided regular polygons of unit side length (dotted line segments), which corresponds to the values in the limit of $\alpha/k_BT\rightarrow\infty$ and which were obtained in the same manner as that for the pairs of rings with finite α/k_BT.

For rings with $(\alpha/k_BT, n)=(0, 1000)$, $(0, 500)$, $(0, 200)$ and $(1, 200)$, whose λL were 1000, 500, 200 and ~ 80, respectively, $\overline{U}_{12}/k_BT$ for a given mixed ensemble was larger than that for the corresponding trivial-knot ensemble; their values themselves and the difference between them become small with decreasing λL. Such behavior of $\overline{U}_{12}(\rho)/k_BT$ may be considered to reflect the density of the bonds constituting the ring around its center of mass. As for the rings with $(\alpha/k_BT, n)=(10, 200)$ and $(100, 200)$, whose λL were ~ 10 and ~ 1, respectively, $\overline{U}_{12}/k_BT$ for the two ensembles become almost identical with each other, because any configurations of nontrivial knots can hardly exist in the mixed ensemble for $\lambda L\lesssim 10$, as seen from Figure 2.

It is interesting to find a dip in $\overline{U}_{12}(\rho)/k_BT$ around $\rho=0$ for the ring with $(\alpha/k_BT, n)=(100, 200)$ and also for the regular polygon. The dip may reflect the fact that the density of the bonds around the center of mass almost vanishes to allow another ring to enter the space. Such behavior of $\overline{U}_{12}/k_BT$ has also been found by Hirayama *et al.*[36] for a self-avoiding polygon and by Bohn and Heermann[37] for a self-avoiding closed path on a simple cubic lattice.

Now we proceed to achieve the purpose of this paper: to examine the behavior of the effective volume V_E or the second virial coefficient A_2 as a function of λL. We numerically calculated $V_{E,mix}$ and $V_{E,t.k.}$ from Equation (1) with Equation (19) with the values of $\overline{U}_{12}/k_BT$ for the mixed and trivial-knot ensembles, respectively. The values of $V_{E,mix}/n^2$ and $V_{E,t.k.}/n^2$ are given in the fourth and sixth columns, respectively, of Table 2, along with their statistical errors. These values and their associated statistical error for given values of α/k_BT and n are the mean and s.d., respectively, of five independent MC results.

Figure 6 shows double-logarithmic plots of $\lambda V_E/L^2$ $(=\lambda V_E/n^2\propto A_2)$ against λL. The open and closed circles represent $\lambda V_{E,mix}/L^2$ and $\lambda V_{E,t.k.}/L^2$, respectively; the various directions of pips carry the same meaning as those in Figure 2. The dotted straight line with unit slope represents the theoretical values for the rigid ring calculated from[7]

$$V_E = L^3/24\pi^2 \quad \text{(rigid ring)}, \tag{23}$$

and the curve associated with the data points for $\lambda V_{E,mix}/L^2$ represents the values calculated from an interpolation formula, which is given below.

The data points for $\lambda V_{E,mix}/L^2$ for various values of α/k_BT seem to form a single-composite curve, which first increases along the dotted

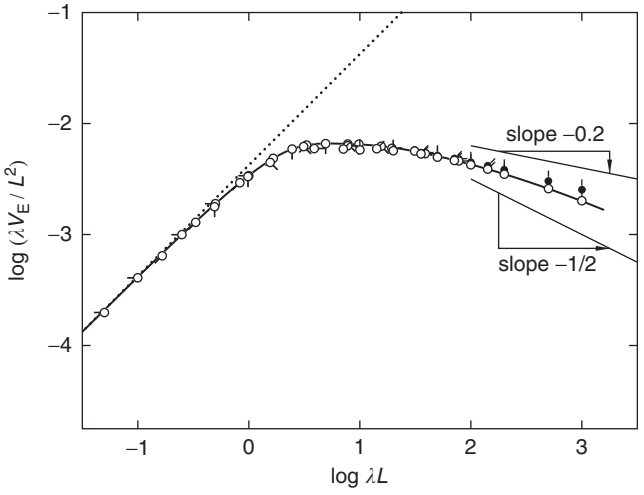

Figure 6 Double-logarithmic plots of $\lambda V_E/L^2$ against λL. The open and closed circles represent the values of $\lambda V_{E,mix}/L^2$ and $\lambda V_{E,t.k.}/L^2$, respectively, with various directions of pips carrying the same meaning as those in Figure 2. The dotted straight line with unit slope represents the theoretical values for the rigid ring[7] and the solid curve represents the values calculated from the interpolation formula for $\lambda V_{E,mix}/L^2$ of the KP ring.

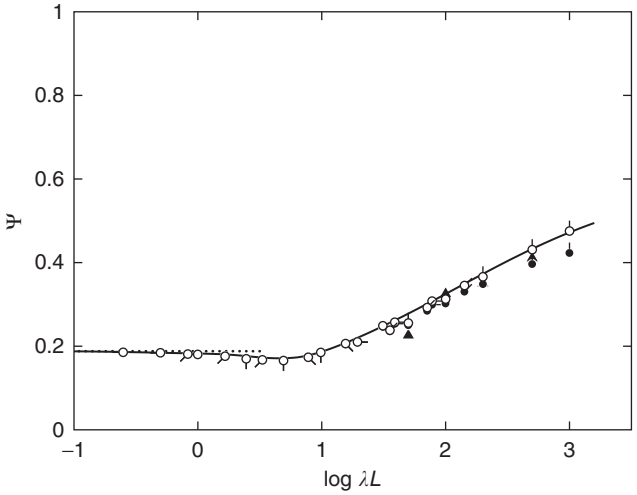

Figure 7 Plots of Ψ against $\log \lambda L$. The open and closed circles represent the values for the mixed and trivial-knot ensembles, respectively, with various directions of pips carrying the same meaning as those in Figure 2. The curve represents the values calculated from the interpolation formula and the dotted horizontal line indicates the asymptotic value $1/3\sqrt{\pi}$ in the rigid-ring limit. The closed triangles represent the values obtained by Deguchi and Tsurusaki[9] for trivial-knot rings.

straight line in the range of $\lambda L \lesssim 0.1$, then deviates downward progressively from the line with increasing λL, and finally decreases after passing through a maximum at $\lambda L \simeq 5$. Each data point for $\lambda V_{E,t.k.}/L^2$ almost completely agrees with the corresponding one for $\lambda V_{E,mix}/L^2$ in the range of $\lambda L \lesssim 10$, where $f_{t.k.} \simeq 1$ and $\langle S^2 \rangle_{t.k.}/\langle S^2 \rangle_{mix} \simeq 1$, and then $\lambda V_{E,t.k.}/L^2$ gradually deviates upward from $\lambda V_{E,mix}/L^2$ with increasing λL. Although $\lambda V_{E,mix}/L^2$ and $\lambda V_{E,t.k.}/L^2$ are considered to become proportional to $L^{-1/2}$ and $L^{-0.2}$, respectively, in the random-coil limit, as mentioned in the introduction, it is difficult to confirm the validity of the exponents on the basis of the present data for $\lambda L \leqslant 10^3$.

From the results shown in Figure 6, $\lambda V_{E,mix}/L^2$ (and also $\lambda V_{E,t.k.}/L^2$) for the (continuous) KP ring without excluded volume may be considered a function only of λL. For convenience, we constructed an interpolation formula for $\lambda V_{E,mix}/L^2$ of the KP ring based on the MC values of $V_{E,mix}/n^2$ for $n \geqslant 100$ given in the fourth column of Table 2 and the asymptotic form (23) in the rigid-ring limit and the asymptotic exponent $-1/2$ in the random-coil limit. We note that the MC values for n=10, 20 and 50 were not used to suppress possible effects of the chain discreteness. The interpolation formula for $\lambda L \lesssim 10^3$ could be given by

$$\lambda V_{E,\,mix}/L^2 = f(\lambda L) \quad \text{for } \lambda L \lesssim 10^3, \tag{24}$$

where

$$f(L) = \frac{L}{24\pi^2}\left[\mathrm{e}^{-0.6014L} + 0.5700L\left(1 + \sum_{i=1}^{4} C_i L^{i/2}\right)^{-1}\right]^{3/2} \tag{25}$$

with the coefficients C_i given by

$$C_1 = 0.9630,\ C_2 = -0.7345,\ C_3 = 0.4887,\ C_4 = 0.07915. \tag{26}$$

The interpolation formula (25) with Equations (26) was accurate within 1%, and the solid curve in Figure 6 represents its values. An asymptotic relation $\lambda V_{E,mix}/L^2 = 0.08_2(\lambda L)^{-1/2}$ in the random-coil limit may be obtained from the formula, although we are uncertain of the accuracy of the factor 0.08_2.

To illustrate the relation of V_E to $\langle S^2 \rangle$, we considered the interpenetration function Ψ defined by[29]

$$A_2 = 4\pi^{3/2} N_A \frac{\langle S^2 \rangle^{3/2}}{M^2} \Psi, \tag{27}$$

which could be calculated from

$$\Psi = \frac{V_E}{(\pi \langle S^2 \rangle)^{3/2}} = \frac{n^{1/2}(V_E/n^2)}{(\pi \langle S^2 \rangle / n)^{3/2}} \tag{28}$$

with the values of $\langle S^2 \rangle / n$ and V_E/n^2 given in Table 2. Figure 7 shows plots of Ψ against the logarithm of λL. The open and closed circles represent the present MC values for the mixed and trivial-knot ensembles, respectively; again, the various directions of pips carry the same meaning as those in Figure 2. We omitted data points for n=10 and 20 from Figure 7 because they were dispersed because of chain discreteness. The dotted horizontal line indicates the asymptotic value $1/3\sqrt{\pi}$ in the rigid-ring limit, which was calculated from Equation (28) with V_E given by Equation (23) and with $\langle S^2 \rangle = L^2/4\pi^2$. The curve represents values calculated from Equation (28) using the interpolation formula for $\lambda V_{E,mix}/L^2$ given by Equations (24)–(26) and $\lambda \langle S^2 \rangle_{mix}/L$ of the KP ring given by Equations (22).

The quantity Ψ for the mixed ensemble deviates slightly downward from the dotted horizontal line with increasing λL for $\lambda L \lesssim 5$ and then increases after passing through a minimum. The quantity Ψ for the trivial-knot ensemble is almost identical to that for the mixed ensemble for $\lambda L \lesssim 10$, as a natural consequence of the behavior of $\lambda \langle S^2 \rangle / L$ and $\lambda V_E/L^2$ shown in Figures 3 and 6; it is then found to gradually deviate downward from the latter with increasing λL. Both quantities may be considered to approach respective asymptotic values in the random-coil limit. Unfortunately, however, we cannot determine the asymptotic values from the MC data for $\lambda L \lesssim 10^3$ but only suppose that the value for the mixed ensemble is larger than that for the trivial-knot ensemble, also in the random-coil limit. We note that an asymptotic value 0.6_1 of Ψ in the random-coil limit may be temporarily estimated for the mixed ensemble from the asymptotic

relations $\lambda V_{E,mix}/L^2=0.08_2(\lambda L)^{-1/2}$ and $\lambda\langle S^2\rangle_{mix}/L=1/12$ mentioned above.

For comparison, Figure 7 shows literature MC data for trivial-knot ensembles (closed triangle) obtained by integrating over ρ of the interpolation formulas for $\overline{U}_{12}(\rho)/k_BT$ constructed by Deguchi and Tsurusaki[9] on the basis of their MC values for rings of the trivial knot composed of n Gaussian springs (n=50, 100, 200 and 500). We note that they adopted more reliable criteria to distinguish knot and link types than ours, that is, the Alexander polynomial and the Vassiliev invariants of degree 2 and 3 used to select trivial-knot rings and the Alexander polynomial for links of two components used to select trivial-link pairs of rings. The present MC values agree with theirs within numerical error, indicating that the criteria adopted in this study work satisfactorily.

Comparison with experiment

Finally, we made a comparison of the present MC results with the experimental ones mentioned in the introduction, where $f(\lambda L)$ given by Equation (25) with Equation (26) as a function of λL is converted into A_2 determined as a function of M_w by

$$\log A_2 = \log[f(\lambda L)] + \log\left(\frac{4N_A\lambda^{-1}}{M_L^2}\right), \tag{29}$$

$$\log M_w = \log(\lambda L) + \log(\lambda^{-1}M_L), \tag{30}$$

where M_L is the shift factor[16] defined as the molecular weight per unit contour length of the corresponding KP ring.

Figure 8 shows double-logarithmic plots of A_2 (in $cm^3\,mol\,g^{-2}$) against M_w. The open circles, squares and triangles represent the experimental values for ring a-PS in cyclohexane at Θ determined from light scattering (LS) measurements by Roovers and Toporowski (at 34.5 °C),[10] by Huang *et al.* (at 35 °C)[11] and by Takano *et al.* (at 34.5 °C),[12] respectively. The curve represents MC values of A_2 calculated from Equation (29) with Equations (25) and (26), with the KP parameter values λ^{-1}=16.8 Å and M_L=35.8 $Å^{-1}$ determined previously from data for $\langle S^2\rangle$ for linear a-PS in cyclohexane at 34.5 °C (Θ).[38] The experimental values obtained by Roovers and Toporowski and by Takano *et al.* agree fairly well with each other (within experimental error), as they stand, but the values obtained by Huang *et al.* are somewhat smaller. In any case, the experimental values are definitely smaller than the MC values, and, therefore, we tried to guess possible causes for the difference.

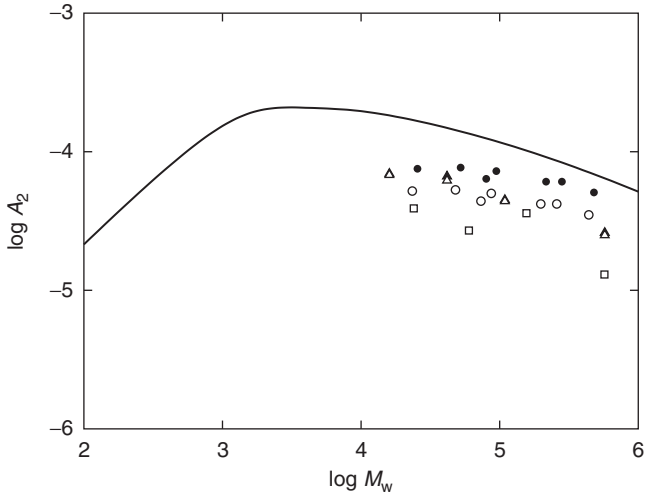

Figure 8 Double-logarithmic plots of A_2 (in $cm^3\,mol\,g^{-2}$) against M_w. The open circles, squares and triangles represent the experimental values for ring a-PS in cyclohexane at Θ by Roovers and Toporowski,[10] by Huang *et al.*[11] and by Takano *et al.*,[12] respectively; the closed symbols represent the corresponding corrected values. The curve represents the MC values calculated from the interpolation formula.

We first measured the effect of contamination by linear residues in the ring a-PS samples synthesized by Roovers and Toporowski,[10] who remarked that the ingredients of the sample with $M_w=5.50\times10^5$, for which A_2 was not determined, were 76 wt% ring polymer with molecular weight $M_{ring}=6.05\times10^5$, 7 wt% residual linear parent polymer with molecular weight M_{ring}, and 17 wt% residual linear polymer with molecular weight $M_{ring}/2$. Applying the LS theory for a solution of heterogeneous polymers,[29,39,40] with the proper assumption that intermolecular interaction vanishes between the linear chains and also between the linear and ring chains, M_{ring} and the second virial coefficient $A_{2,ring}$ for a solution only of ring a-PS may be related to observed M_w and A_2 by $M_{ring}=1.09\,M_w$ and $A_{2,ring}=1.45\,A_2$, respectively (see Appendix). If the ingredients of all the samples shown in Figure 8 are assumed to be the same as those mentioned above, the data points represented by the open circles in Figure 8 may be replaced by the closed circles. For the samples synthesized by Takano *et al.*,[12] the weight fraction w of residual linear polymer having the same M_w as that of the corresponding ring polymer was evaluated to be 1.0, 3.4, 1.0 and 2.0 wt% for samples with $M_w=1.6\times10^4$, 4.17×10^4, 1.09×10^5 and 5.73×10^5, respectively. For the solutions of such samples, $A_{2,ring}$ may be related to observed A_2 by $A_{2,ring}=w^{-2}\,A_2$, and M_w remains unchanged (see Appendix). The closed triangles in Figure 8 represent the corrected values. As for the samples synthesized by Huang *et al.*,[11] no information was given about residual linear polymers. As seen from Figure 8, the corrected data points seem rather dispersed. Some experimental problems remain to be resolved.

Theoretically, on the other hand, it should be remarked that the present MC model takes account of only the TI between a pair of rings but not of the interaction between the segments constituting the real ring polymers (that is, the ordinary excluded-volume effect). The residual contribution of three-segment interactions[41] on A_2 remains even at Θ, where the effective binary-cluster integral and, therefore, A_2 for linear polymer with very large M vanish;[29] A_2 remains slightly negative (up to order $10^{-5}\,cm^3\,mol\,g^{-2}$) at Θ if M is not very large.[38,42,43] The residual contribution must, to some extent, decrease the theoretical value of A_2. Furthermore, there is no information about knot types of ring polymers included in a given test sample (that is, about whether or not the configurations of the ring polymers in the sample are of all kinds of knots with the Boltzmann weight). If rather complicated knots happen to be preferred, $\langle S^2\rangle$ and, therefore, A_2 may become smaller than the respective values for the mixed ensemble.

Apart from the unresolved discrepancy in the A_2 value of order $10^{-5}\,cm^3\,mol\,g^{-2}$, the present MC results in Figure 8 combined with the values of the KP model parameters previously determined may qualitatively explain the behavior of the experimental data. The most important implication of Figures 6–8 is that the ring a-PS in the range of $1\times10^4\lesssim M_w\lesssim6\times10^5$ is still far from the random-coil limit.

CONCLUSION

The second virial coefficient A_2 of the KP ring without excluded volume, resulting only from the TI, was evaluated based on the present MC results; also, its behavior was examined as a function of the reduced total contour length λL in the range of the crossover from the rigid ring to the random coil. The reduced quantity $\lambda V_E/L^2$

proportional to A_2 was shown to be a function only of λL, which first increases along the values of the rigid ring ($\propto L$) and then decreases after passing through a maximum at $\lambda L \simeq 5$ as λL is increased. Although $\lambda V_E/L^2$ was considered to become proportional to $(\lambda L)^{-1/2}$ for a mixed ensemble of configurations of all kinds of knots with the Boltzmann weight and to $(\lambda L)^{-0.2}$ for the trivial-knot ensemble, in the random-coil limit of $\lambda L \to \infty$, the range of $\lambda L \leqslant 10^3$ (where MC simulations were actually carried out) does not yet enter in the limit and cannot directly confirm the asymptotic relations. The present results with the values of the KP model parameters determined previously allow for a qualitative explanation of the behavior of the available literature data for ring a-PS in cyclohexane at Θ, and clearly show that the range of $M_w \lesssim 6\times10^5$ (where the experiments were actually carried out) is still far from the random-coil limit. Quantitatively, however, there is a discrepancy in the A_2 value of order $10^{-5}\,\mathrm{cm^3\,mol\,g^{-2}}$, causes of which seem to lie on both the theoretical and the experimental sides.

1 Edwards, S. F. Statistical mechanics with topological constraints: I. *Proc. Phys. Soc.* **91,** 513–519 (1967).
2 Edwards, S. F. Statistical mechanics with topological constraints: II. *J. Phys. A* **1,** 15–28 (1968).
3 Vologodskii, A. V., Lukashin, A. V. & Frank-Kamenetskii, M. D. Topological interaction between polymer chains. *Zh. Eksp. Teor. Fiz.* **67,** 1875–1885 (1974)[*Soviet Phys. JETP* **40**, 932–936 (1975)].
4 Frank-Kamenetskii, M. D., Lukashin, A. V. & Vologodskii, A. V. Statistical mechanics and topology of polymer chains. *Nature* **258,** 398–402 (1975).
5 Iwata, K. & Kimura, T. Topological distribution functions and the second virial coefficients of ring polymers. *J. Chem. Phys.* **74,** 2039–2048 (1981).
6 Iwata, K. Evidence of topological interaction among polymers: A_2 of ring polymers in the Θ-state. *Macromolecules* **18,** 115–116 (1985).
7 des Cloizeaux, J. Ring polymers in solution: topological effects. *J. Phys. Lett.* **42,** L-433–L-436 (1981).
8 Tanaka, F. Osmotic pressure of ring-polymer solutions. *J. Chem. Phys.* **87,** 4201–4206 (1987).
9 Deguchi, T. & Tsurusaki, K. Random knots and links and applications to polymer physics. *Proc. Lect. Knots* **96,** 95–122 (1997).
10 Roovers, J. & Toporowski, P. M. Synthesis of high molecular weight ring polystyrenes. *Macromolecules* **16,** 843–849 (1983).
11 Huang, J., Shen, J., Li, C. & Liu, D. A new theoretical approach to problems of the solution behavior of ring-shaped polymers. *Makromol. Chem.* **192,** 1249–1254 (1991).
12 Takano, A., Kushida, Y., Ohta, Y., Matsuoka, K. & Matsushita, Y. The second virial coefficients of highly-purified ring polystyrenes. *Polymer* **50,** 1300–1303 (2009).
13 Grosberg, A. Y. Critical exponents for random knots. *Phys. Rev. Lett.* **85,** 3858–3861 (2000).
14 Moore, N. T., Lua, R. C. & Grosberg, A. Y. Topologically driven swelling of a polymer loop. *Proc. Natl. Acad. Sci. USA* **101,** 13431–13435 (2004).
15 Kratky, O. & Porod, G. Röntgenuntersuchung gelöster fadenmoleküle. *Recl. Trav. Chim. Pay-Bas.* **68,** 1106–1122 (1949).
16 Yamakawa, H. *Helical Wormlike Chains in Polymer Solutions* (Springer, Berlin, 1997).
17 Frank-Kamenetskii, M. D., Lukashin, A. V., Anshelevich, V. V. & Vologodskii, A. V. Torsional and bending rigidity of the double helix from data on small DNA rings. *J. Biomol. Struct. Dynam.* **2,** 1005–1012 (1985).
18 Shimada, J. & Yamakawa, H. Moments for DNA topoisomers: the helical wormlike chain. *Biopolymers* **27,** 657–673 (1988).
19 Deutsch, J. M. Equilibrium size of large ring molecules. *Phys. Rev. E.* **59,** R2539–R2541 (1999).
20 Yamakawa, H. & Yoshizaki, T. A Monte Carlo study of effects of chain stiffness and chain ends on dilute solution behavior of polymers. I. Gyration-radius expansion factor. *J. Chem. Phys.* **118,** 2911–2918 (2003).
21 Metropolis, N., Rosenbluth, A. W., Rosenbluth, M. N., Teller, A. H. & Teller, E. Equation of state calculations by fast computing machines. *J. Chem. Phys.* **21,** 1087–1092 (1953).
22 Vologodskii, A. V., Lukashin, A. V., Frank-Kamenetskii, M. D. & Anshelevich, V. V. The knot problem in statistical mechanics of polymer chains. *Zh. Eksp. Teor. Fiz.* **66,** 2153–2163 (1974)[*Soviet Phys. JETP* **39**, 1059–1063 (1974)].
23 Crowell, R. H. & Fox, R. H. *Introduction to Knot Theory* (Ginn, Boston, 1963).
24 Kinoshita, S. & Terasaka, H. On unions of knots. *Osaka Math. J.* **9,** 131–153 (1957).
25 Matsumoto, M. & Nishimura, T. Mersenne Twister: a 623-dimensionally equidistributed uniform pseudo-random number generator. *ACM Trans. Model. Comput. Simul.* **8,** 3–30 (1998), see also the URL:http://www.math.sci.hiroshima-u.ac.jp/~m-mat/MT/emt.html.
26 Rolfsen, D. *Knots and Links* (Publish or Perish, Berkeley, 1976).
27 Klenin, K. & Langowski, J. Computation of writhe in modeling of supercoiled DNA. *Biopolymers* **54,** 307–317 (2000).
28 McMillan, W. G. & Mayer, J. E. The statistical thermodynamics of multicomponent systems. *J. Chem. Phys.* **13,** 276–305 (1945).
29 Yamakawa, H. *Modern Theory of Polymer Solutions* (Harper & Row, New York, 1971). Available at:http://www.molsci.polym.kyoto-u.ac.jp/archives/redbook.pdf.
30 Kontsevich, M. Vassiliev's knot invariants. *Adv. Soviet Math.* **16,** 137–150 (1993).
31 Diao, Y., Pippenger, N. & Sumners, D. W. On random knots. *J. Knot Theory Ramif.* **3,** 419–429 (1994).
32 Diao, Y. The knotting of equilateral polygons in R^3. *J. Knot Theory Ramif.* **4,** 189–196 (1995).
33 Fujii, M. & Yamakawa, H. Moments and transport coefficients of wormlike rings. *Macromolecules* **8,** 792–799 (1975).
34 Kramers, H. A. The behavior of macromolecules in inhomogeneous flow. *J. Chem. Phys.* **14,** 415–424 (1946).
35 Zimm, B. H. & Stockmayer, W. H. The dimensions of chain molecules containing branches and rings. *J. Chem. Phys.* **17,** 1301–1314 (1949).
36 Hirayama, N., Tsurusaki, K. & Deguchi, T. Linking probabilities of off-lattice self-avoiding polygons and the effects of excluded volume. *J. Phys. A: Math. Theor.* **42,** 105001-1–105001-18 (2009).
37 Bohn, M. & Heermann, D. W. Topological interactions between ring polymers: implications for chromatin loops. *J. Chem. Phys.* **132,** 044904-1–044904-10 (2010).
38 Yamakawa, H. & Yoshizaki, T. A Monte Carlo study of effects of chain stiffness and chain ends on dilute solution behavior of polymers. II. Second virial coefficient. *J. Chem. Phys.* **119,** 1257–1270 (2003).
39 Kirkwood, J. G. & Goldberg, R. J. Light scattering arising from composition fluctuations in multi-component systems. *J. Chem. Phys.* **18,** 54–57 (1950).
40 Stockmayer, W. H. Light scattering in multi-component systems. *J. Chem. Phys.* **18,** 58–61 (1950).
41 Yamakawa, H. Three-parameter theory of dilute polymer solution. *J. Chem. Phys.* **45,** 2606–2617 (1966).
42 Cherayil, B. J., Douglas, J. F. & Freed, K. F. Effect of residual interactions on polymer properties near the theta point. *J. Chem. Phys.* **83,** 5293–5310 (1985).
43 Nakamura, Y., Norisuye, T. & Teramoto, A. Second and third virial coefficients for polystyrene in cyclohexane near the Θ point. *Macromolecules* **24,** 4904–4908 (1991).

APPENDIX

Effects of residual linear polymers on A_2 at Θ

Consider a solution of heterogeneous polymers in a single solvent, and let M_i be the molecular weight of polymer species i (i=1, 2, ⋯, r), w_i be its weight fraction in the whole polymer, and c be the whole concentration. The excess scattering R_θ determined from LS measurements for the solution may then be expanded in powers of c as follows,[29,39,40]

$$Kc/R_\theta = M_w^{-1} + 2A_{2,LS}c + \cdots, \tag{A.1}$$

where K is the optical constant and $A_{2,LS}$ is the second virial coefficient determined from LS defined by

$$A_{2,LS} = M_w^{-2} \sum_{i=1}^{r} \sum_{j=1}^{r} M_i M_j A_{ij} w_i w_j. \tag{A.2}$$

In Equation (A.2), the coefficient A_{ij} ($=A_{ij}$) may be related to the effective volume excluded to a polymer chain of species i by the presence of another of species j and is defined by

$$A_{ij} = -\frac{N_A}{2VM_iM_j} \int [F_2(i,j) - F_1(i)F_1(j)]\mathrm{d}(i,j), \tag{A.3}$$

where $F_2(i, j)$ is the two-body distribution function of a pair of polymer chains of species i and j, and $F_1(i)$ is the one-body distribution function of a polymer chain of species i. We note that A_{ii} is identical with $A_{2,LS}$ for a solution only of polymer species i. We also note that M_w is explicitly given by

$$M_w = \sum_{i=1}^{r} w_i M_i. \tag{A.4}$$

For a solution of a ring polymer (species 1) and linear polymers (species 2, 3, $\cdots$) composed of identical repeat units, all the coefficients A_{ij} except $A_{11}=A_{2,\mathrm{ring}}$, vanish at Θ for the solution of only the linear polymers. For the solution of the sample synthesized by Roovers and Toporowski,[10] we set $r=3$, $M_1=M_2=M_{\mathrm{ring}}$, $M_3=M_{\mathrm{ring}}/2$, $w_1=0.76$, $w_2=0.07$ and $w_3=0.17$ in Equations (A.2) and (A.4) to obtain $A_{2,\mathrm{ring}}=1.45A_{2,\mathrm{LS}}$ and $M_{\mathrm{ring}}=1.09M_{\mathrm{w}}$, respectively. As for the solutions of the samples synthesized by Takano *et al.*,[12] we set $r=2$, $M_1=M_2=M_{\mathrm{ring}}$, $w_1=w$ and $w_2=1-w$ in Equations (A.2) and (A.4) to obtain $A_{2,\mathrm{ring}}=w^{-2}A_{2,\mathrm{ring}}$ and $M_{\mathrm{ring}}=M_{\mathrm{w}}$, respectively.